PROCEEDINGS, 50th Workshop on Geothermal Reservoir Engineering
Stanford University, Stanford, California, February 10-12, 2025
SGP-TR-229

# Estimation of the Average Soil Thermal Conductivity and Grout Thermal Resistance from the Thermal Response Test using Nonlinear Regression

Rodney Hurt, Kevwe Andrew Ejenakevwe, Li Song, and Xingru Wu*

The University of Oklahoma, Norman, OK 73019

rodney.d.hurt-1@ou.edu, kevwe.ejenakevwe@ou.edu, lsong@ou.edu, xingru.wu@ou.edu*

*Corresponding Author

**Keywords:** Thermal Conductivity, Thermal Resistance, Nonlinear Regression,

## ABSTRACT

The thermal response test (TRT) is often used to determine the in-situ thermal conductivity of soil for a geothermal heat pump, which uses the constant temperature of the shallow earth to exchange heat efficiently. A conventional TRT takes about 50 hours or longer to see the straight-line relationship between the temperature and logarithm of elapsed time. This practice is easy to use but takes a long time to test, is costly, and results in limited information. Furthermore, this practice requires the input thermal power to be constant, which is often a challenge in reality. We propose a new set of TRT data interpretations by analyzing the whole transient thermal transfer regime to obtain the thermal conductivity and diffusivity of soil and thermal resistance of grout of the test well.

In the TRT process, the thermal disturbance propagates away from the borehole as heated working fluid circulates through the borehole. At early test times, the measured temperature behavior is affected by the grout properties used in cementing the borehole. Thermal conductivity is not constant over the borehole lifespan as it ages. In a relatively long testing period, the measured temperature behavior is mainly affected by the soil thermal diffusivity, which can be characterized by the integral exponential function. A logarithm approximation can be applied in lieu of the integral exponential function once the test reaches a sufficient duration. Conventional TRT analysis only uses data in the late stage and discards previous measurements. Our method utilizes the whole testing period and uses nonlinear regression to match the measurements and determine the model parameters including grout thermal resistance, thermal diffusivity and conductivity of the soil.

In the paper, we first discuss the fundamentals of TRT and its analysis. Then we apply the method to show the procedure of interpretation using the new method. The application of the real case shows that our approach is robust in theory, accurate in modeling, and able to determine more parameters by thoroughly using the measurements.

## 1. INTRODUCTION

Geothermal or ground source heat pumps (GSHPs) operate by rejecting/absorbing heat to/from the soil. When a GSHP is in operation, working fluid is pumped through the heat pump to one or more ground heat exchangers or wells. The system harnesses the stable temperature of the earth to transfer heat, significantly reducing the reliance on fossil fuels for building climate control. Unlike traditional heating systems, which often involve natural gas or oil combustion, GSHPs use electricity to operate, which can be sourced from renewable energy, further decreasing greenhouse gas emissions. By utilizing the earth's constant temperature, the heat pump efficiency, known as the coefficient of performance (COP), is maintained higher than air cooled systems. COP is given as

$$COP = \frac{Heat\ Transferred\ [W]}{Power\ Input\ [W]} \tag{1}$$

In addition to their decarbonization benefits, geothermal and GSHP systems improve energy efficiency by minimizing energy losses inherent in conventional systems. For example, during heating, they extract heat from the ground rather than generating it or extracting heat from the ambient air, leading to lower energy consumption. Similarly, they release heat into the ground in cooling, which is more efficient than dissipating it into the air. GSHPs offer a few benefits over traditional air source heat pumps (ASHPs). GSHPs have more consistent heating and cooling output over the course of a year than ASHPs. The heating and cooling output is highly affected by the outdoor air temperature. This reduced energy demand lowers operational costs and alleviates pressure on electrical grids, especially during peak demand periods. Furthermore, GSHPs can contribute to a building's net-zero energy goals when integrated with other renewable energy sources, such as solar panels, creating a synergistic pathway toward sustainable energy use.

Figure 1 shows the typical operational performance of an air source heat pump. GSHPs have similar performance curves except the x-axis variable (ambient temperature) would be replaced with the carrier fluid temperature. Cooling efficiency reduces with higher outdoor air temperatures, and heating efficiency reduces with lower outdoor air temperatures. Heating output and heating COP are both highlighted in yellow. The heating output can drop to 40% of the design rating or lower as outdoor air temperature decreases.

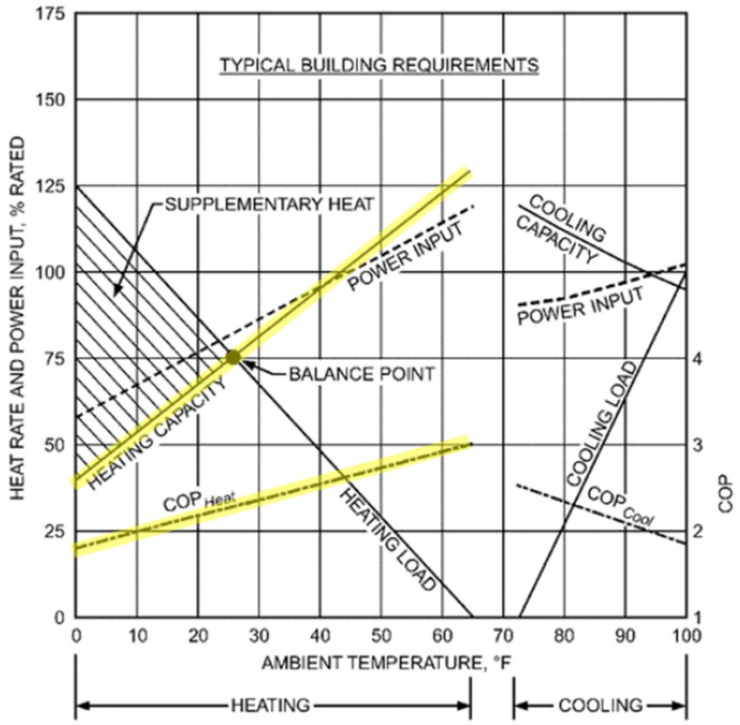


**Figure 1: Typical ASHP operating performance (ASHRAE 2020)**

Oklahoma climatic design conditions dictate outdoor air temperature of 26.6°F (-3°C) for heating and 98.6°F (37°C) for cooling, encompassing weather conditions for 99% of the time (ASHRAE 2021). This results in a heating output of approximately 75% of the design rating and a COP (efficiency) reduction of 24%. This means that the heat pump will have to run longer to maintain comfort conditions or may fail to maintain them entirely, resulting in increased energy consumption and cost. Compare these results to those of a GSHP, which has a much narrower operating temperature range due to the thermal stability of the soil. For example, Montagud (et al. 2012) recorded fluid return temperatures ranging from 60.8°F to 79.7°F (16°C to 26.5°C) over 25 years. Figure 2 shows that soil temperature past a certain depth becomes practically constant (Omer 2008). GSHP fluid return temperatures will vary based on location, bore geometry, and netload. However, GSHPs will nearly always result in more consistent operating conditions and higher performance than ASHPs in the same area.


**Figure 2: Air and soil temperature comparison (Omer 2008)**

Soil temperature at a certain depth beyond the range of surface effects will remain constant, as in Omer. However, the soil temperature will change once heat transfer is introduced like with a GSHP system. Li (et al. 2015) found that the bore wall temperature can change by

as much as 74°F (23.32 °C) with a constant heat injection of 41.6 $\frac{Btu}{hr-ft}$ (40 $\frac{W}{m}$ )over a period of 5 years. Positive heat injection as in this study, is analogous to a cooling-dominated building load where heat is injected into the ground. The soil and carrier fluid temperature will rise over time in this scenario. The heat pump cooling output and cooling efficiency will decrease over time. If the net load of the well were negative, e.g., in a heating-dominated building, the soil temperature would reduce along with heating output and efficiency. Therefore, it is critical to have accurate soil thermal properties for borehole design.

The thermal efficiency of a GSHP is highly affected by the thermal conductivity coefficient of the soil in contact with the wellbore. The thermal conductivity coefficient is affected by soil minerals, voidage ratio, in-situ fluid flow condition, and moisture contents. These parameters vary from site to site and even along the same borehole. The orientation of the well(s) will affect the heat transfer efficiency and capacity. They can be installed vertically or horizontally with one or more wells per system. Vertical bores for use with GSHP systems generally range from 100 to 500 ft (30.5 to 152.4 m) in depth. This study focuses on a single real-world, vertical well.

Accurately measuring the in-situ thermal conductivity along the borehole is critical to designing a geothermal application. This study will introduce the thermal response test (TRT), which was developed to determine effective thermal conductivity over the whole length of the borehole. TRT results are interpreted using the traditional infinite line source model using steady-state results after approximately 40 hours. The results are also interpreted using the entire dataset, which includes both transient and steady-state results. The resulting soil thermal conductivity, thermal diffusivity, and borehole equivalent thermal resistance vary slightly between the methods. However, both results are closely matched to the measured temperature response. The transient temperature response begins yielding results after a shorter period

## 2. THEORY OF ESTIMATING IN-SITU HEAT CONDUCTIVITY

Several interpretation algorithms have been developed based on the line source model with different solution methods such as the infinite line, finite line, and infinite cylindrical method (Zhang et al. 2019). parameters estimations may vary because each method applies different assumptions to solve for unknown. The infinite line source model is typically used with the thermal response test. This method starts by assuming heat transfer is driven by the temperature difference between the average temperature of the heat carrier fluid and the average borehole wall temperature. Equation 2 gives the average fluid temperature based on measurable points.

$$T_f = 0.5(T_i + T_e) \tag{2}$$

where $T_f, T_i,$ and $T_e$ are the average fluid temperature, fluid inlet temperature, and fluid exit temperature, respectively. The temperature of the borehole wall, $T_b$, is estimated by introducing the borehole thermal resistance, $R_b$, and is given by:

$$T_f - T_b = R_b q_E \tag{3}$$

where $R_b$, $q_E$ are respectively the thermal resistance of the borehole in $\frac{K-m}{W}$, heat flux per unit length, $\frac{W}{m}$.

The infinite line source model neglects the borehole dimensions with the assumption that heat transfer occurs from an infinitesimally thin line extending infinitely into the earth. The temperature variation between the circulating fluid and the ground can be obtained with Equation 4:

$$\frac{2\pi\lambda}{q_E}\left[T_b(t) - T_g\right] = -\frac{1}{2}E_i\left(-\frac{r_b^2}{4\alpha t}\right) \tag{4}$$

where $\lambda, T_g, r_b, \alpha, t$ are the soil thermal conductivity, soil temperature at far-field, borehole radius, thermal diffusivity, and time, respectively.

The soil temperature from the wellbore to the constant far field temperature, $T_g$, is transient in time. An exponential integral function can be used to relate the temperatures in the infinite line source model. When $\frac{r_b^2}{4\alpha t} < 0.01$ or $t > \frac{(5r_b)^2}{\alpha}$, a logarithm can be used to approximate the exponential integral function as follows (Gehlin 2002):

$$E_i\left(-\frac{r_b^2}{4\alpha t}\right) = ln\left(\frac{4\alpha t}{r_b^2}\right) - \gamma \tag{5}$$

where

$$\gamma = Euler's\ constant, \sim 0.57722\ldots$$

The logarithmic approximation requires that the TRT run for sufficient time for accurate results. For example, a borehole with a radius of 0.03 ft (0.1 m), and soil thermal diffusivity of $9.7 \times 10^{-6}\ ft^2/s$ ($9 \times 10^{-7}\ m^2/s$) requires a minimum test duration of 77 hours. A smaller borehole radius takes significantly longer duration to achieve similar approximation result. Austin III recommended a minimum duration of 50 hours based on their experience with field data sets. Gehlin (1998, 2002) suggests a minimum duration of 60 h but recommends 72 h. From the above discussion, the minimum duration depends on the soil thermal diffusivity and the borehole geometry.

Inserting the logarithm expression into Equation 5 and rearranging it gives:

$$T_b(t) = \frac{q_E}{4\pi\lambda}\left[ln\left(\frac{4\alpha t}{r_b^2}\right) - \gamma\right] + T_g \tag{6}$$

To relate the measured temperature, $T_f$, Equation (2) is inserted into Equation (6) to give:

$$T_f = R_b q_E + \frac{q_E}{4\pi\lambda}\left[ln\left(\frac{4\alpha t}{r_b^2}\right) - \gamma\right] + T_g \tag{7}$$

Equation (7) can be rearranged into an alternate solution for a simpler solution.

$$T_f = R_b q_E + \frac{q_E}{4\pi\lambda}\left[ln(t) + ln\left(\frac{4\alpha}{e^{\gamma} r_b^2}\right)\right] + T_g \tag{8}$$

Equation (8) can be represented as a straight-line equation with $T_f$ as the dependent variable, $In(t)$ as the independent variable, a slope (m) and an intercept (b) given by Equations (9) and (10):

$$m = \frac{q_E}{4\pi\lambda} \tag{9}$$

$$b = R_b q_E + m\, ln\left(\frac{4\alpha}{e^{\gamma} r_b^2}\right) + T_g \tag{10}$$

The thermal diffusivity, α, is given as

$$\alpha = \frac{\lambda}{\rho c_p} = \frac{\lambda}{M_R} \tag{11}$$

From Equations (10) and (11), $b = f(R_b, M_R)$ and implies that with $b$ and either $R_b$ or $M_R$, the other property can be gotten.

Furthermore, from Equations (3), (6), and (8), $R_b$ can be expressed as:

$$R_b = \frac{1}{q_E}\left(T_f - T_g\right) - \frac{1}{4\pi\lambda}\left[\ln(t) + \ln\left(\frac{4\alpha}{e^{\gamma} r_b^2}\right)\right] \tag{12}$$

For convenience, $R_b$ and α can be solved at the intercept (where t=1).

$$R_b = \frac{b - T_g}{q_E} - \frac{m}{q_E} ln\left(\frac{4\alpha}{e^{\gamma} r_b^2}\right) \tag{13}$$

$$\alpha = \frac{r_b^2}{4} exp\left[\gamma + \frac{b - T_g - R_b q_E}{m}\right] \tag{14}$$

Several assumptions have been made in the above derivation.

1. The borehole is vertical
2. Homogeneous thermal properties in the entire vertical session
3. Borehole heat transfer is in a steady state, and from the borehole to the far field is a transient state.
4. The test duration is sufficiently long to use the logarithm approximation.
5. The wellbore is assumed to be a line source.
6. The injection of thermal power is constant.

We can see two shortcomings of the above conventional methods. First, it requires the injection thermal power to be constant, which is hard to achieve in reality. Figure 4 shows the measured power output from the generator and input into the well normalized by the well depth. Secondly, most measured data points are abandoned given the logarithm approximation requirement, as previously discussed.

Alternatively, the thermal diffusivity equation can be solved without the logarithmic approximation constraints for a borehole with a finite radius when heat injection is constant. The cylindrical source solution in the Laplace domain is given by:

$$\bar{T}_D(r_D, s) = \frac{K_o\left(\sqrt{s} r_D\right)}{s^{1.5} K_1\left(\sqrt{s}\right)} \tag{15}$$

Where s is the Laplace variable, $K_0\ and\ K_1$ are modified Bessel functions of the second kind, and $\bar{T}$ is the dimensionless wellbore temperature. The Stehfest Inverse Laplace Transform is applied to convert to the time domain. The dimensionless temperature is

equivalent to the left-hand side of Equation 4. Given this relationship, the bore temperature and fluid temperature can be derived in the same way as shown in Equations 6-8. Non-linear regression is used to obtain the in-situ thermal conductivity coefficient of soil, borehole equivalent resistance, and thermal diffusivity of soil simultaneously. This solution improves overall accuracy, e.g. reduces the root mean square error (RMSE), as it uses the entire dataset rather than exclusively the late stage.

## 3. A TRT CASE STUDY

The TRT was conducted on an existing vertical ground heat exchanger located in Shawnee, OK. The test was conducted by a local geothermal testing company for a 48-hour period starting on January 30, 2024. This test involves pumping carrier fluid through the ground heat exchanger and an external heating unit. Heat is supplied to the system at a constant rate. The flow rate is set to ensure that the temperature differential between entering and exiting fluid is held steady between 6 and 12 °F (3.5 and 7 °C).

The TRT aims to determine the in-situ thermal conductivity of the site. The borehole tested was in operation with a heat pump, and the borehole was estimated at 5.75 in in diameter and 450 feet in depth. It has a 1 in SDR-11 4710 HDPE loop and the borehole is grouted with standard bentonite grout to the surface. Figure 3 gives a schematic illustration of the TRT.

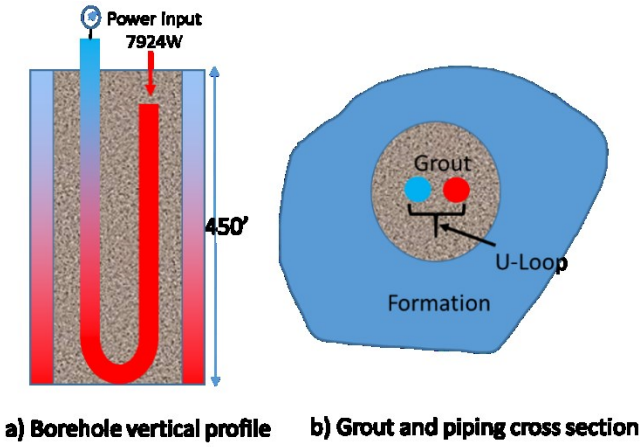


**Figure 3: Diagram of borehole cross sections of the testing well. The injection thermal power was kept at approximately 7924 W in the 48-hour test.**

The power input averaged 7924.7 W and ranged from 7622 W to 7951 W. Variations in power input are due to equipment limitations. However, the effects of slight power deviations can be minimized because power was measured at each timestep which can be considered in the thermal conductivity calculation.

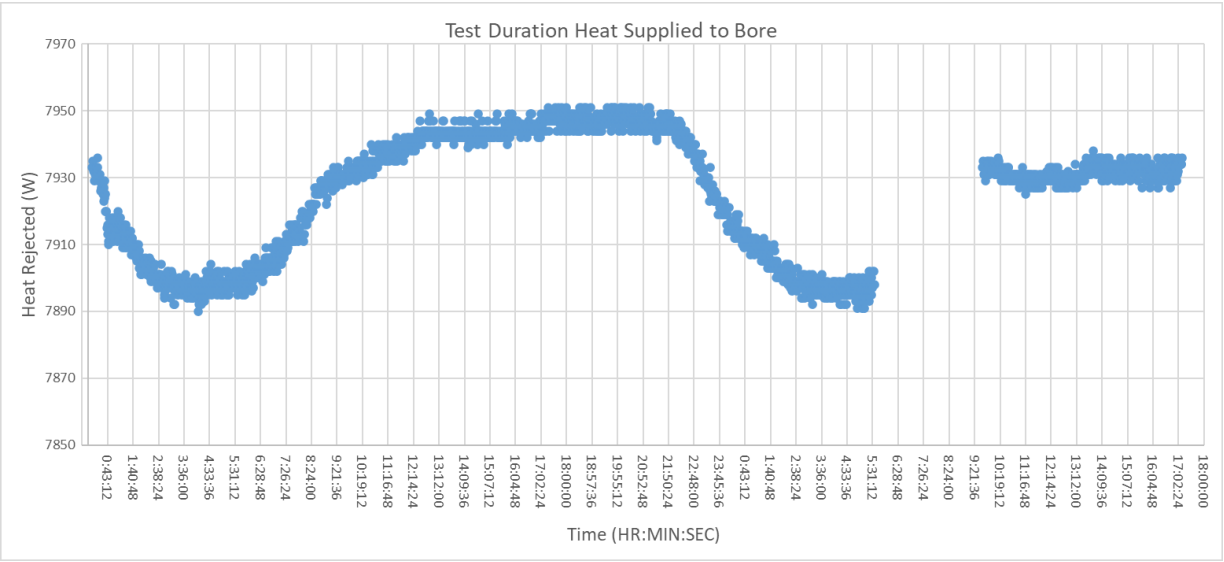


**Figure 4: Recorded power input over test duration**

The temperatures at the inlet and outlet were recorded every 60 seconds for the test duration. Inlet (entering), outlet (leaving), and the calculated average temperatures for the test duration are shown in Figure 5. The fluid temperatures rise quickly in the first few hours as

the grout in the well and adjacent soil temperature increase from their initial conditions. At approximately 8 hours, a transition period occurs in which the temperature change with respect to time becomes more linear. At approximately 28 hours into the test, the temperature change is linear enough for traditional line source methods to be used. These times are approximations based on this specific test. The general trends will be seen in other thermal response tests, but the timeline will be affected by borehole geometry, grout material, and local soil conditions.

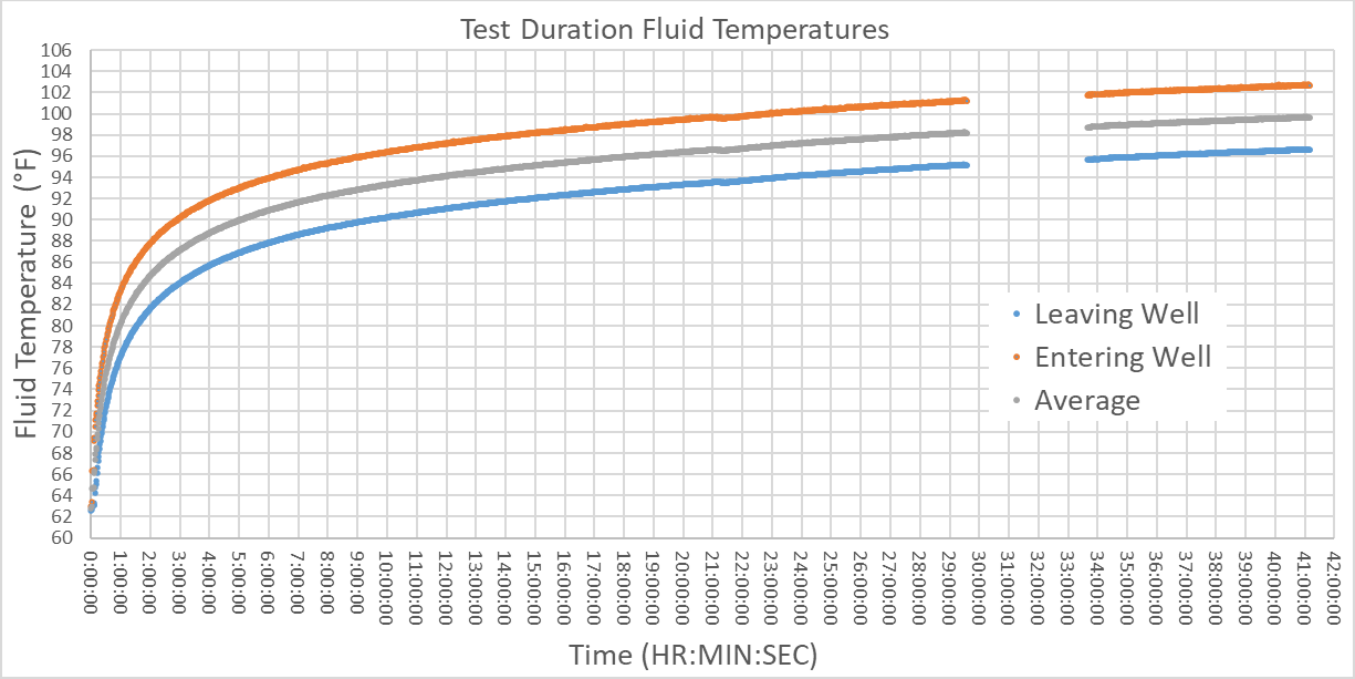


**Figure 5: Recorded inlet, outlet, and average fluid temperature during the test; the gap in the figure is missing data for unknown reasons from the operator.**

The geothermal gradient in this site is about $1.54 \times 10^{-2}\ °F/ft$ ($2.81 \times 10^{-2}\ K/m$) based on the Oklahoma Geological Survey map shown in Figure 3 (Luza et al. 1984). It is necessary to consider the gradient as the far field soil temperature increases with depth, which affects the heat transfer rate from the well. The near-surface soil temperature was measured during testing at 64 °F (17.8 °C). These two conditions allow for the far field surface temperature to be calculated along the depth of the well.

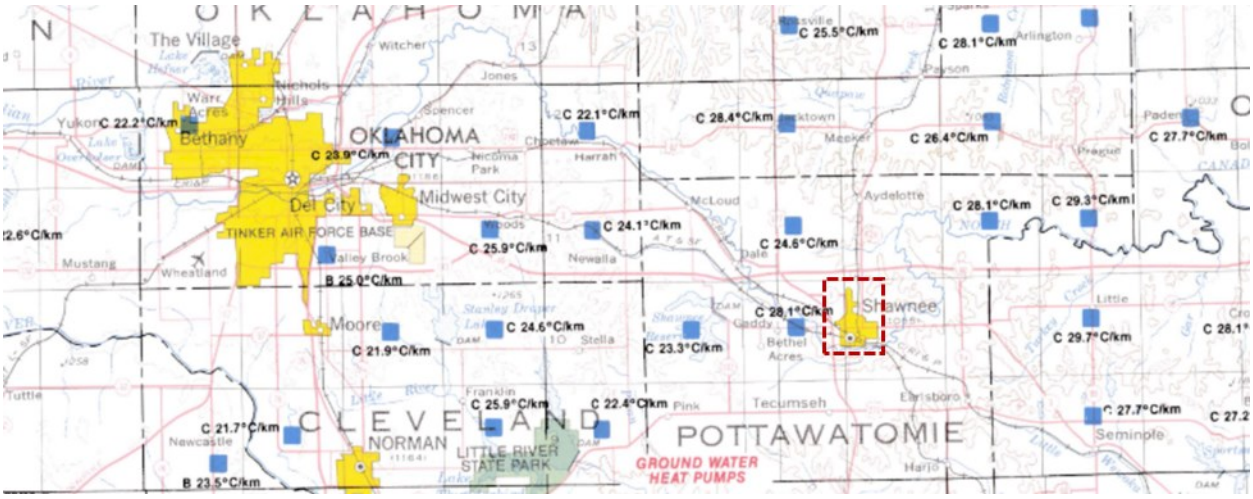


**Figure 6:Geothermal temperature gradient Oklahoma, test area in red, Oklahoma Geological Survey (Luza et al. 1984)**

## 4. RESULTS

Section 4.1 includes the results of the logarithmic approximation. Section 4.2 contains the inverse Laplace transform results, and Section 4.3 compares results of the two methods.

### 4.1 Logarithmic Approximation Results

The logarithmic approximation of the exponential integral function ($E_i$) was applied to measurements taken after 40 hours in the test. This method yields the thermal conductivity of soil as 1.06 $\frac{BTU}{hr-ft-°F}$, the thermal diffusivity as $2.88 \times 10^{-2} \frac{ft^2}{hr}$, and borehole equivalent resistance as $0.281 \frac{ft-°F-hr}{BTU}$. Figure 8 shows the calculated temperature over the entire test duration compared to the measured data. For clarity, the parameter estimation only used measured data after 40 hours, but the figure shows the full dataset.

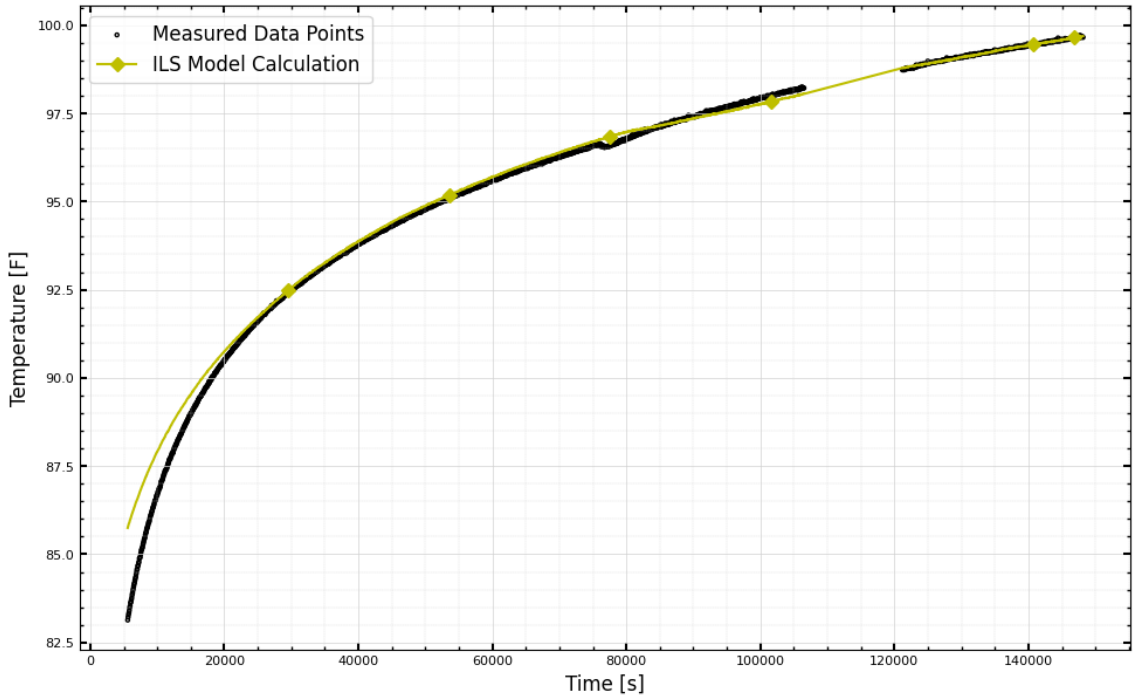


**Figure 7: Logarithmic approximation of fluid temperature**

The resulting fluid temperature is most accurate in the final steady state range which is expected because that is the only time period in which the parameters were trained. Error is greatest in the initial steady state phase. These results show that the traditional interpretation method does require the TRT to be conducted until temperature change becomes linear for a sufficient time. The test had to be greater than 40 hours for this well.

### 4.2 Inverse Laplace Transform Parameter Estimation

This section contains the results of the inverse Laplace transformation and nonlinear regression using the entire dataset. This method results in the thermal conductivity coefficient of soil as 0.98 $\frac{BTU}{hr-ft-°F}$, borehole equivalent resistance as 0.26 $\frac{ft-°F-hr}{BTU}$, and the soil thermal diffusivity coefficient as $2.90 \times 10^{-2} \frac{ft^2}{hr}$. In addition to estimating the parameters using the entire dataset, other estimations were calculated for shorter test durations at 18 and 28 hours. Figure 8 shows the fluid temperature calculated with each set of estimated parameters.

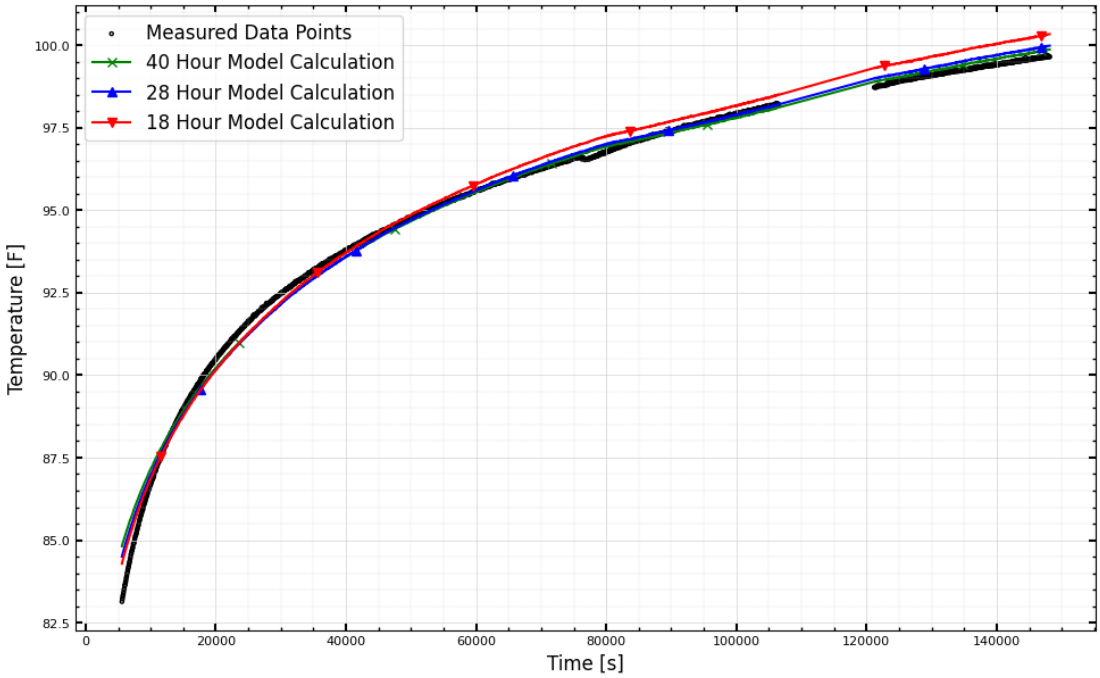


**Figure 8: Fluid temperature comparison using multiple test durations**

Error for all estimations is largest at the initial data point but quickly follows the trend of the measured data. The 18 hour estimation results in the largest error, which is to be expected. However, it still follows the trend well and has a maximum error of 1.2°F. Results of the 28-hour and 40-hour estimation have even higher accuracy. The RMSE of each is 0.378, 0.248, and 0.253 for the 18-hour, 28-hour, and 40-hour tests, respectively. This shows that satisfactory parameter estimations may be attainable even earlier than 40 hours.

### 4.3 Result Comparison

Both data interpretation methods yielded similar results but with significantly different test duration datasets. Table 1 provides soil parameters from the inverse Laplace Transform estimation and comparisons with the logarithmic approximation results.

**Table 1：Calculated and assumed parameters**

| Properties | Value | Unit | Sources | Comments |
|---|---|---|---|---|
| Soil thermal conductivity | 0.983 [1.69] | $\frac{BTU}{hr-ft-°F}\left[\frac{W}{m-K}\right]$ | 40-hour Thermal response test | Logarithm approximation estimation is 1.041 $\frac{BTU}{hr-ft-°F}$ |
| Soil thermal diffusivity | 0.029 [0.0027] | $\frac{ft^2}{hr}\left[\frac{m^2}{hr}\right]$ | 40-hour Thermal response test | |
| Soil specific heat capacity | 0.269 [1125.2] | $\frac{BTU}{lb-°F}\left[\frac{J}{kg-K}\right]$ | 40-hour Thermal response test and literature | Determined using the estimated conductivity, diffusivity, and Equation (11) with a density to specific heat ratio of approximately 460. Compared with 0.292* $\frac{BTU}{lb-°F}$. (Gehlin 2002) and 149 $\frac{lbm}{ft^3}$ for sandstone (Dalla Santa et al. 2020)<br>*Converted from volumetric heat capacity |
| Soil density | 124.9 [2000.71] | $\frac{lbm}{ft^3}\left[\frac{kg}{m^3}\right]$ | 40-hour Thermal response test and literature | |

| | | | | |
|---|---|---|---|---|
| Grout conductivity | 0.463 [0.8] | $\frac{BTU}{hr-ft-°F}\left[\frac{W}{m-K}\right]$ | 40-hour Thermal response test | Compared with 0.46 $\frac{BTU}{hr-ft-°F}$ and 0.587 $\frac{BTU}{hr-ft-°F}$. (Kurevija et al. 2017, Mahmoud et al. 2021) |
| Grout-specific heat capacity | 0.597 [2500.0] | $\frac{BTU}{lb-°F}\left[\frac{J}{kg-K}\right]$ | Thermal response test | Compared with 0.610* $\frac{BTU}{lb-°F}$. (Naldi et al. 2021)<br>*Converted from volumetric heat capacity |
| Grout density | 112.4 [1800.5] | $\frac{lbm}{ft^3}\left[\frac{kg}{m^3}\right]$ | Literature | (Mahmoud et al. 2021, Delaleux et al. 2012) |

Local data suggests that the soil type is predominately silt/sand. Calculated results compared with the typical report of soil thermal properties in Table 2 (Dalla Santa et al. 2020) show that the measured heat conductivity coefficient along the wellbore is much higher than that of the soil description. The following argument can explain this. First, the estimated value is an average of 450' interval. The heat conductivity coefficient typically increases as the soil is compacted. Secondly, the aquifer is active in the measurement site, and the water table is reported below 15-35' below the surface. Heat convection could dominate when an active aquifer surrounds the borehole, significantly increasing the apparent heat conductivity coefficient.

**Table 2: Typical thermal conductivity values of different soil types (Dalla Santa et al. 2020)**

| | **Thermal Conductivity $\frac{BTU}{hr-ft-°F}\left[\frac{W}{m-K}\right]$** | | |
|---|---|---|---|
| **Sediment category** | **Min-value** | **Max-value** | **Recommended value** |
| **Gravel dry** | 0.232 [0.4] | 0.522 [0.9] | 0.232 [0.4] |
| **Gravel water-saturated** | 0.928 [1.6] | 1.45 [2.5] | 1.044 [1.8] |
| **Sand dry** | 0.174 [0.3] | 0.522 [0.9] | 0.232 [0.4] |
| **Sand moist** | 0.58 [1] | 1.102 [1.9] | 0.812 [1.4] |
| **Sand water-saturated** | 1.16 [2] | 1.74 [3] | 1.392 [2.4] |
| **Clay/silt dry** | 0.232 [0.4] | 0.58 [1] | 0.29 [0.5] |
| **Clay/silt water-saturated** | 0.638 [1.1] | 1.798 [3.1] | 1.044 [1.8] |
| **Till/loam** | 0.638 [1.1] | 1.682 [2.9] | 1.392 [2.4] |
| **Peat, soft lignite** | 0.116 [0.2] | 0.406 [0.7] | 0.232 [0.4] |

As discussed in Section 4.2, The parameters can be identified in even shorter amounts of time with differing degrees of error. Table 3 shows select results of different test durations.

**Table 3: Parameter estimates at different test durations**

| Training Data Range | Soil Thermal Conductivity $\frac{BTU}{hr-ft-°F}\left[\frac{W}{m-K}\right]$ | Borehole Equivalent Thermal Resistance $\frac{ft-°F-hr}{BTU}\left[\frac{m-K}{W}\right]$ | Soil Thermal Diffusivity $\frac{ft^2}{hr}\left[\frac{m^2}{hr}\right]$ |
|---|---|---|---|
| 18 hours | 0.896 [1.545] | 0.269 [0.269] | 0.0203 [0.0019] |
| 28 hours | 0.96 [1.655] | 0.255 [0.255] | 0.0287 [0.0027] |
| 40 hours | 0.977 [1.684] | 0.258 [0.258] | 0.029 [0.0027] |
| Linear Temperature Change (33.6-41.2 hrs) | 1.06 [1.828] | 0.281 [0.281] | 0.0289 [0.0027] |

The soil conductivity estimation is 8.3% and 1.7% less than the final 40-hour value after only 18 and 28 hours, respectively. The equivalent resistance is off by -4.5% and 1.0% after the same duration. Lastly, the soil thermal diffusivity is off the final value by 30% and 1.3% at

those points. Based on these observations, a borehole of this geometry can be identified in approximately 28 hours, as opposed to 40 or more hours.

The difference in error between each test duration, including only using steady state, can be explained by which data and how much data is used for the regression. The performance of each set of results can be compared based on the calculated fluid temperature using the respective parameters as shown in Figure 9.

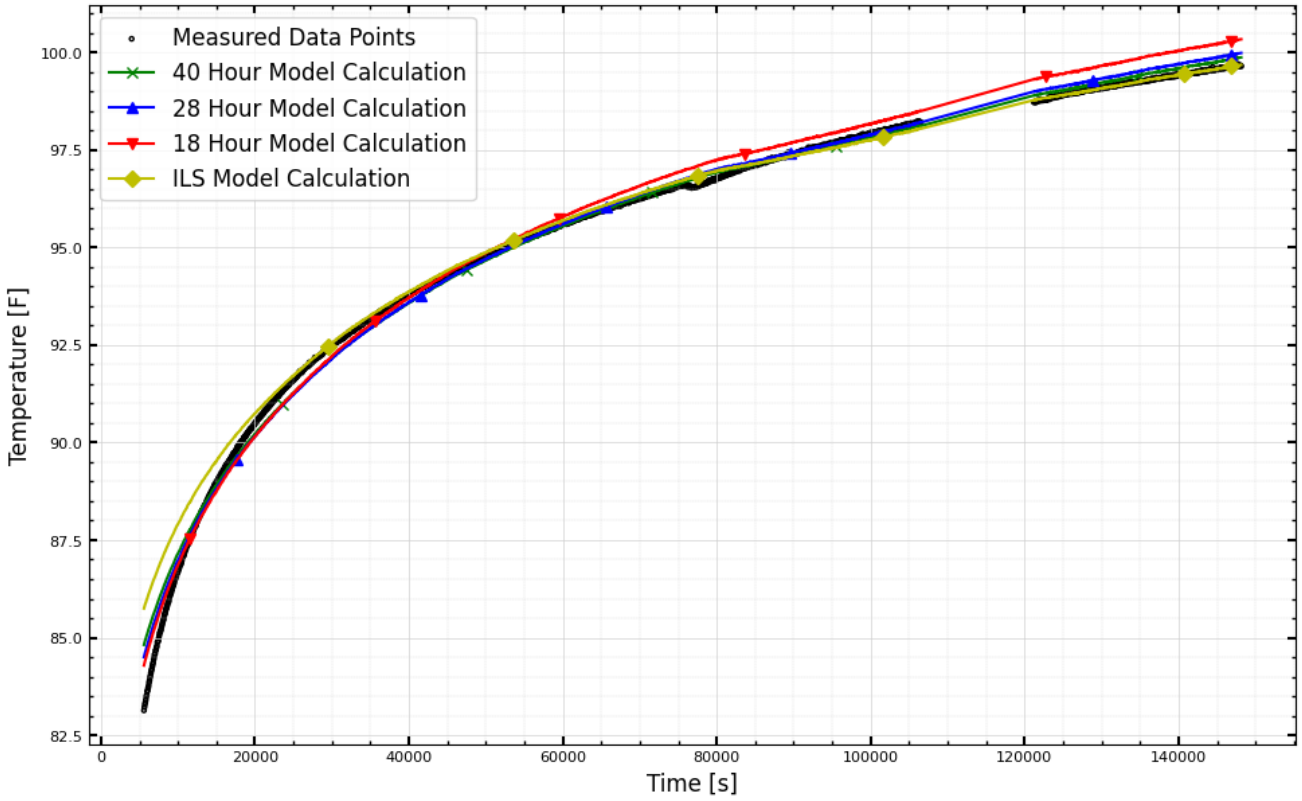


**Figure 9: Fluid temperature comparison**

In addition to the temperature response in Figure 9, it is beneficial to observe the overall error of each estimation. Table 4 gives the root mean square error (RMSE) of each test. First, the error is calculated from data over the entire test duration, then by only considering the error during linear temperature change (33.6-41.2 hrs). The 28-hour test actually performs the highest based on the complete dataset. However, it suffers when highlighting the linear temperature change stage error. The traditional logarithmic approximation has the lowest error in the steady state period but has poor performance over the complete dataset. This is to be expected as the parameters were trained on that data exclusively.

**Table 4: Fluid temperature root mean square error**

| Training Data Range | Complete Test Duration | Linear Temperature Change Duration (33.6-41.2 hrs) |
|---|---|---|
| 18 hours | 0.378 | 0.599 |
| 28 hours | 0.248 | 0.266 |
| 40 hours | 0.253 | 0.159 |
| Linear Temperature Change (33.6-41.2 hrs) | 0.405 | 0.022 |

Including the early duration temperature response reduces the overall error as expected, although linear temperature change performance is impacted. The inverse Laplace transform method captures the fluid temperature dynamics more effectively than the traditional method when considering the entire test duration.

## 6. CONCLUSIONS

Accurately predicting the soil thermal conductivity is critical in designing wells for ground source heat pump systems. Improperly designed wells can result in reduced heat pump output and efficiency. Inadequate bore geometry and spacing can also lead to temperature saturation in the soil, where the temperature increases over time. Eventually, the soil temperature will exceed the air temperature, resulting in worse cooling performance than an ASHP.

The infinite line source model typically used in conjunction with a thermal response test offers accurate results. However, the test must be conducted for a considerable amount of time. Generally, it takes at least 50 hours, but that time can increase based on the local soil properties and the bore geometry. The proposed inverse Laplace transform TRT interpretation makes use of the entire dataset. This can reduce the overall test time and improve result accuracy. Calculated results for soil thermal diffusivity, conductivity, and borehole equivalent resistance are within reasonable values compared with real-world measurements after 28 hours on this dataset.

## REFERENCES

Sanner, B., et al. *Thermal response test–current status and world-wide application*. in *Proceedings world geothermal congress*. 2005. Citeseer.

Raymond, J., et al., *A review of thermal response test analysis using pumping test concepts.* Groundwater, 2011. **49**(6): p. 932-945.

Zhang, X., et al., *Comparison of four methods for borehole heat exchanger sizing subject to thermal response test parameter estimation.* Energies, 2019. **12**(21): p. 4067.

Gehlin, S., *Thermal response test: method development and evaluation*. 2002, Luleå tekniska universitet.

Austin III, W.A., *Development of an in situ system for measuring ground thermal properties*. 1998, Oklahoma State University.

Gehlin, S., *Thermal response test: in situ measurements of thermal properties in hard rock*. 1998, Luleå tekniska universitet.

Stehfest, H., *Algorithm 368: Numerical inversion of Laplace transforms [D5].* Communications of the ACM, 1970. **13**(1): p. 47-49.

Kurevija, T., M. Macenić, and S. Borović, *Impact of grout thermal conductivity on the long-term efficiency of the ground-source heat pump system.* Sustainable Cities and Society, 2017. **31**: p. 1-11.

Mahmoud, M., et al., *A review of grout materials in geothermal energy applications.* International Journal of Thermofluids, 2021. **10**: p. 100070.

Delaleux, F., et al., *Enhancement of geothermal borehole heat exchangers performances by improvement of bentonite grouts conductivity.* Applied Thermal Engineering, 2012. **33**: p. 92-99.

American Society of Heating, Refrigerating and Air-Conditioning Engineers, Inc. (ASHRAE). (2020). 2020 ASHRAE Handbook - HVAC Systems and Equipment (I-P Edition). American Society of Heating, Refrigerating and Air-Conditioning Engineers, Inc. (ASHRAE).

"ASHRAE Climatic Design Conditions." *ASHRAE Climatic Design Conditions 2009/2013/2017/2021*, ASHRAE (American Society of Heating Refrigerating and Air Conditioning Engineers), 2021, ashrae-meteo.info/v2.0/.

Montagud, Carla, et al. "Experimental and modeling analysis of a ground source heat pump system." *Applied Energy*, vol. 109, 11 Dec. 2012, pp. 328–336, https://doi.org/10.1016/j.apenergy.2012.11.025.

Mustafa Omer, Abdeen. "Ground-source heat pumps systems and applications." *Renewable and Sustainable Energy Reviews*, vol. 12, no. 2, Feb. 2008, pp. 344–371, https://doi.org/10.1016/j.rser.2006.10.003.

Luza, Kenneth V., et al. "GM-27 Geothermal Resources and Temperature Gradients of Oklahoma." *Geothermal Resources and Temperature Gradients of Oklahoma*, Oklahoma Geological Survey, 1984.

Dalla Santa, Giorgia, et al. "An updated ground thermal properties database for GSHP applications." *Geothermics*, vol. 85, May 2020, https://doi.org/10.1016/j.geothermics.2019.101758.

Li, Chaofeng, et al. "Analysis of geo-temperature restoration performance under intermittent operation of borehole heat exchanger fields." *Sustainability*, vol. 8, no. 1, 31 Dec. 2015, p. 35, https://doi.org/10.3390/su8010035.

Naldi, Claudia, et al. "A new estimate of Sand and grout thermal properties in the sandbox experiment for accurate validations of borehole simulation codes." *Energies*, vol. 14, no. 4, 21 Feb. 2021, p. 1149, https://doi.org/10.3390/en14041149.